

**Preliminary results of
lidar based studies of
the aerosol vertical
distribution in the lower
troposphere over urban
coastal areas**

OCEANOLOGIA, 46 (3), 2004.
pp. 347–364.

© 2004, by Institute of
Oceanology PAS.

KEYWORDS

Aerosol
Vertical profile
Urban area
Lidar

MAREK HAŁAS¹
ZDZISŁAW BŁASZCZAK¹
JÓZEF GRABOWSKI²
ALEXANDROS PAPAYANNIS³
TYMON ZIELIŃSKI⁴

¹ Optics Division,
Faculty of Physics,
A. Mickiewicz University,
Umultowska 85, PL–60–614 Poznań, Poland;
e-mail: halas@amu.edu.pl

² Institute of Physics,
Technical University,
Nieszawska 13a, PL–60–965 Poznań, Poland

³ Department of Physics,
Technical University of Athens, Athens, Greece

⁴ Institute of Oceanology,
Polish Academy of Sciences,
Powstańców Warszawy 55, PL–81–712 Sopot, Poland

Manuscript received 29 July 2004, reviewed 10 August 2004, accepted 16 August 2004.

Abstract

The paper reports the results of lidar measurements performed in the lower troposphere during several measurement sessions in Athens (Greece) in 2000. For the sake of comparison, results of a similar study performed in Kołobrzeg (Poland) in 2001 are also given. These data indicate that the exhaust gases produced by motor transportation in the cities resulted in the formation of an inversion layer. The rate of convection of the inversion layer depends on the intensity of sunlight,

The complete text of the paper is available at <http://www.iopan.gda.pl/oceanologia/>

the strength of winds and the morphology of the land. The inversion layer reaches the highest altitudes in the middle of summer, lower in early and late summer and the lowest in autumn. Over the sea the inversion layer altitude extends to several meters, but on moving inland it rises to a few hundred meters.

1. Introduction

The broad scope of problems related to environmental protection includes those relating to the protection of the atmosphere, the state of which has proved vital to what happens on the ground. The commonly used methods for monitoring atmospheric pollution (including aerosols) are optical ones, which collect data from a given point or a small area (Resso & Harris 1989, Mims 1992, Labow et al. 1996, Dixon 1998, Drollette 2000, Heintzenberg et al. 2003). Very important among them are the lidar methods based on the use of pulse or continuous lasers as they are characterized by high sensitivity and a long range of penetration. Lidars are mobile and can thus be used at different sites, including satellites (Hoppel et al. 1985, Ailisto et al. 1996, Wilczak et al. 1996, Brinkmann 1999, Mody 1999, Robinson 2001, Voss et al. 2001, Kunz et al. 2002, Hong et al. 2004). Lidar measurements permit a highly accurate determination of the type and size of pollutants, even at long distances, are able to detect aerosols of very low concentrations, and allow a study of their spatio-temporal dynamics. By employing several wavelengths the lidar provides very accurate information about the size distribution of aerosol particles as well as their concentrations under various weather conditions and at different altitudes above sea level (Monahan et al. 1983, Monahan & Mac Niocaill 1986, Wu 1992).

Characterization of the real atmosphere requires a large number of meteorological parameters such as temperature, humidity, wind directions, and in addition, variations in chemical composition and the presence of pollutants, which can undergo rapid local changes, in particular over urban areas. Models of the real atmosphere require many parameters based on a large number of observational data. The design of very accurate models is limited by computer capacity, so in practice simplified models are used.

This paper presents the analyses of lidar data collected on selected days in 2000 in Athens (Greece) (Błaszczak et al. 2003a, b). For comparison, the results collected in Kołobrzeg (Poland) in 2001 using the FLS-12 lidar (Błaszczak et al. 2003a, b) are also discussed.

2. Lidar data processing technique

The lidar data were analyzed by the general iteration method (Klett 1985, Grabowski & Papayannis 1999a, b), also known as the general recurrence method proposed by Klett (1985). The recurrence of the lidar

data starts from the points farthest from the ground, usually at an altitude of about 10 km, where the effect of the aerosol's presence can be neglected. At this altitude it is possible, on the basis of the extinction coefficient and backscattering for a single point, to calculate the general values of these parameters and the lidar ratio (formula 3) for aerosols from the lower troposphere.

2.1. The general lidar equation

The differential lidar equation takes the form

$$\frac{dS}{dr} = \frac{1}{\beta(r)} \frac{d\beta(r)}{dr} - 2\alpha(r), \quad (1)$$

where β is the backscattering coefficient and α is the extinction coefficient at distance r . The experimental value of the corrected lidar signal denoted by S is

$$S(r) = [r^2 P(r)], \quad (2)$$

where r is the distance from the source of radiation, and $P(r)$ is the power of the signal recorded by the detector (Measures 1984). Eq. (1) proposed by Klett (1985) is solved following the introduction of constant C_2 , known as the lidar ratio. C_2 is defined as the ratio of the backscattering coefficient to the extinction coefficient. Since both these coefficients have a common dependence on the distance r , the lidar constant is independent of r :

$$C_2 = \frac{\beta(r)}{\alpha(r)}. \quad (3)$$

However, the analysis of a large number of experimental data has indicated that the lidar ratio does depend on the light wavelength and air humidity (Salemink et al. 1984, Kovalev 1993) as well as on the altitude a.s.l.

The expression for $\beta(c)$ involving a value of C_2 that is dependent on r is given by

$$\beta(r) = C_2(r)\alpha(r). \quad (4)$$

The derivative over altitude is

$$\frac{d\beta(r)}{dr} = C_2(r) \frac{d\alpha(r)}{dr} + \alpha(r) \frac{dC_2(r)}{dr}, \quad (5)$$

in which the lidar constant C_2 depends on the altitude (Klett 1985, Grabowski & Papayannis 1999a, b).

The solutions of the above equation are the values of a and β given in discrete form by the sums

$$\alpha(r) = \frac{\exp \left[S(r) - S(r_f) - \ln \frac{C_2(r)}{C_2(r_f)} \right]}{\frac{1}{\alpha(r_f)} + 2 \sum_{r_f - n\Delta r}^{r_f} \left[S(r) - S(r_f) - \ln \frac{C_2(r)}{C_2(r_f)} \right] \Delta r}, \quad (6)$$

and

$$\beta(r) = \frac{\exp[S(r) - S(r_f)]}{\frac{1}{\beta(r_f)} + 2 \sum_{r_f - n\Delta r}^{r_f} \frac{\exp[S(r) - S(r_f)]}{C_2(r)} \Delta r}. \quad (7)$$

The values with the index f refer to the point farthest from the observer, where the atmosphere is assumed to consist solely of gas molecules. Eqs. (6) and (7) give the values of the extinction and backscattering coefficients for an atmosphere containing aerosols and air molecules. For aerosols, the extinction and backscattering coefficients α_a and β_a are obtained as

$$\alpha_a(r) = \alpha(r) - \alpha_m(r), \quad (8)$$

$$\beta_a(r) = \beta(r) - \beta_m(r), \quad (9)$$

where the index a refers to aerosols and m to the molecular atmosphere. Consequently, eqs. (6) and (7) for aerosol particles can be written as

$$\alpha_a(r) = \frac{\exp \left[S(r) - S(r_f) - \ln \frac{C_2(r)}{C_{2m}} \right]}{\frac{1}{\alpha_m(r_f)} + 2 \sum_{r_f - n\Delta r}^{r_f} \left[S(r) - S(r_f) - \ln \frac{C_2(r)}{C_{2m}} \right] \Delta r} - \alpha_m(r), \quad (10)$$

and

$$\beta_a(r) = \frac{\exp[S(r) - S(r_f)]}{\frac{1}{\beta_m(r_f)} + 2 \sum_{r_f - n\Delta r}^{r_f} \frac{\exp[S(r) - S(r_f)]}{C_2(r)} \Delta r} - \beta_m(r), \quad (11)$$

and the lidar ratio is

$$C_{2a}(r) = \frac{\beta_a(r)}{\alpha_a(r)}. \quad (12)$$

The form of this equation is very suitable for numerical calculations of the lidar ratio for the farthest to the nearest points to the observer, and then for determining the extinction and backscattering coefficients of aerosols.

For the analysis of the lidar data the following assumptions were made: $S = 10$ and $\Delta S = 10^{-4}$; $\beta = 10^{-4} \text{ m}^{-1} \text{ sr}^{-1}$; $\alpha = 10^{-3} \text{ m}^{-1}$; $C_2 = 0.05$ and $\Delta C_2 = 0.0001$; $C_{2m} = 0.05$ and $\Delta C_{2m} = 0.0001$; $\beta(r_f) = \beta_{\text{molecular}}(r_f) = 10^{-5} \text{ m}^{-1} \text{ sr}^{-1}$ and $\Delta\beta(r_f) = 10^{-9} \text{ m}^{-1} \text{ sr}^{-1}$; $\alpha(r_f) = \alpha_{\text{molecular}}(r_f) = 10^{-4} \text{ m}^{-1}$ and $\Delta\alpha(r_f) = 10^{-8} \text{ m}^{-1}$; $\Delta r = 15 \text{ m}$.

The derivation of the errors in $\alpha(r)$ in eq. (10) involves the use of the partial derivative of the following formula:

$$\Delta\alpha = \frac{d\alpha}{dS}\Delta S + \frac{d\alpha}{d\alpha_m}\Delta\alpha_m \frac{d\alpha}{dC_2}\Delta C_2 + \frac{d\alpha}{dC_{2m}}\Delta C_{2m}, \quad (13)$$

which yields the following values:

$$\left. \frac{d\alpha}{dS} \right|_{\substack{\alpha_m = \text{const} \\ C_2 = \text{const} \\ C_{2m} = \text{const}}} = 10^{-4}; \quad \left. \frac{d\alpha}{d\alpha_m} \right|_{\substack{S = \text{const} \\ C_2 = \text{const} \\ C_{2m} = \text{const}}} = 1; \quad \left. \frac{d\alpha}{dC_2} \right|_{\substack{S = \text{const} \\ \alpha_m = \text{const} \\ C_{2m} = \text{const}}} = 10^{-3} \quad \text{and}$$

$$\left. \frac{d\alpha}{dC_{2m}} \right|_{\substack{S = \text{const} \\ \alpha_m = \text{const} \\ C_2 = \text{const}}} = 10^{-3}.$$

The partial derivatives and the assumed values yielded a value of $\Delta\alpha$ of the order of 10^{-8} .

Error analysis for the coefficient $\beta(r)$ from formula (11) involves calculating the partial derivatives of the following formula:

$$\Delta\beta = \frac{d\beta}{dS}\Delta S + \frac{d\beta}{dC_2}\Delta C_2 + \frac{d\beta}{d\beta_m}\Delta\beta_m, \quad (14)$$

and they are:

$$\left. \frac{d\beta}{dS} \right|_{\substack{C_2 = \text{const} \\ \beta_m = \text{const}}} = 10^{-5}; \quad \left. \frac{d\beta}{dC_2} \right|_{\substack{S = \text{const} \\ \beta_m = \text{const}}} = 10^{-8}; \quad \left. \frac{d\beta}{d\beta_m} \right|_{\substack{S = \text{const} \\ C_2 = \text{const}}} = 1.$$

The partial derivatives and the assumed values yielded a value of $\Delta\beta$ of the order of 10^{-9} .

The pollution concentration formula $C = \frac{\alpha}{2\pi r^2}$, where the radius r is of the order of 10^{-7} m , and Δr is of the order of 10^{-8} m , yields the concentration at a level of 10^{10} . Thus the concentration uncertainty from the partial derivatives is described as follows:

$$\Delta C = \frac{dC}{d\alpha}\Delta\alpha + \frac{dC}{dr}\Delta r, \quad (15)$$

and

$$\left. \frac{dC}{d\alpha} \right|_{r = \text{const}} = 10^{14} \quad \text{while} \quad \left. \frac{dC}{dr} \right|_{\alpha = \text{const}} = 10^{17}.$$

The partial derivatives and the assumed values yielded a value of ΔC of the order of 10^9 . The uncertainty in the concentration value is at the level of 10% of the total concentration; thus the impact of the measurement errors on the corrected signals was insignificant. However, certain systematic measurement uncertainties related to the calculations of the maximum values were analyzed in the SigmaPlot software. Using these results, the backscattering ratio uncertainty was estimated at about 10%. A detailed description of the error analyses was presented by Marengo et al. (1997).

2.2. Experimental setup

The experimental setup operated by the Faculty of Physics, Technical University of Athens, worked with a light source provided by a beam from an Nd:YAG laser made by Quantel, and its second (532 nm) and third (355 nm) harmonics (Fig. 1). The light beams were emitted parallel to the axis of the receiving telescope at a distance of 45 cm from this axis. A Newtonian telescope 30 cm in diameter focused the scattered light in an optical fiber through which it was fed to a detection system. In this system a set of filters separated the radiation of 355 nm and 532 nm and directed it to the multichannel photomultipliers (Hamamatsu).

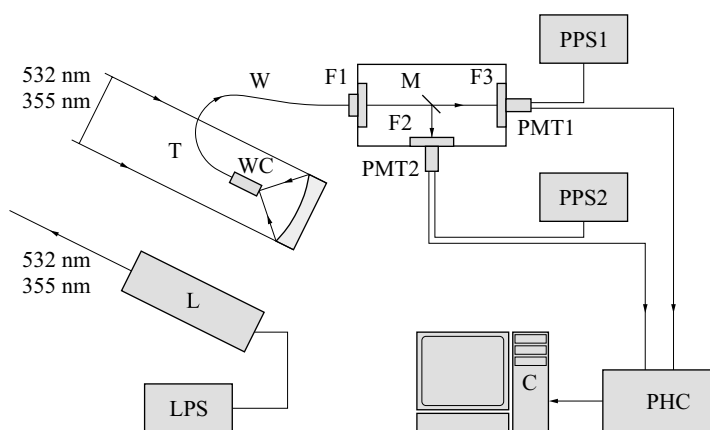


Fig. 1. The experimental lidar system designed and constructed at the Faculty of Physics, Athens Polytechnic, (T – telescope, WC – light waveguide connection, W – light waveguide, F1, F2 and F3 – narrow band interface filters, PMT1 and PMT2 – photomultipliers, PPS1 and PPS2 – photomultiplier power supply systems, PHC – photon counter, C – PC unit, L – laser Nd:YAG, LPS – laser power supply)

The electric signal was amplified, converted to a digital one, and then stored in a computer. The laser generated light pulses of nanosecond duration and energy of the order of 0.41 KJ at a frequency of 10 Hz. The scattered light signals recorded within 6 minutes in one measuring session were composed of a few thousand pixels for a single measurement point. Depending on the time of recording by the detection system the average time corresponding to the distance between the measuring points, was 50 ns, which gave a resolution of 7.5 m. The high output energy of the laser enabled the pollution to be studied at a distance of up to 10 kilometers. However, the signal coming from long distances was very weak, so the measurements were usually performed up to 5–6 kilometers away.

The results of the measurements performed using the FLS-12 lidar from the IO PAS complement the results obtained in Athens, since the aerosols in the Baltic coastal zone were measured from sea level to a height of a few hundred meters, while in the coastal zone of the Mediterranean sea – from a height of a few hundred meters to a few kilometers. In the presence of strong onshore winds, aerosols occur at low levels both in Athens and in Kołobrzeg.

The FLS-12 lidar (Fig. 2) used by the Air-Sea Interaction Laboratory of the Institute of Oceanology PAS in Sopot is a tuneable laser system designed for remotely sensing the air in the VIS spectrum range (320–670 nm). The source of UV pumping for the dye laser is a XeCl excimer laser (308 nm). During the experiments the lidar collected aerosol backscattering data every 50 ns, that is every 7.5 m on the optical path,

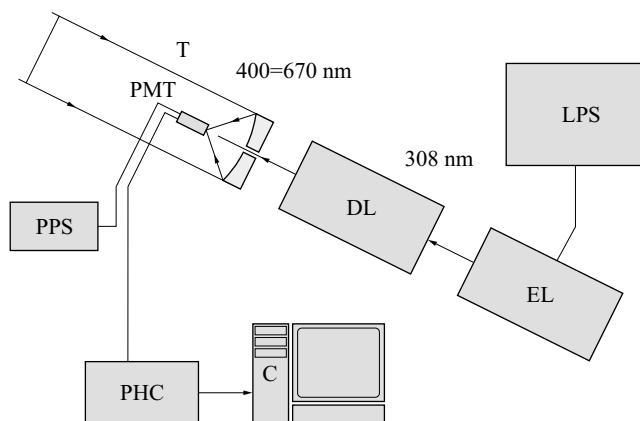


Fig. 2. A diagram of the FLS-12 lidar from the Institute of Oceanology, Polish Academy of Sciences, Sopot (T – telescope, PMT – photomultiplier, PPS – photomultiplier power supply, PHC – photon counter, C – PC unit, EL – excimer laser, DL – dye laser, LPS – excimer laser power supply)

and three wavelengths of 430 nm, 560 nm and 670 nm were employed. The useful part of the optical path was between 60 and 1500 m and altitudes up to 500 m were sampled. The scattered signal was recorded by a Cassegranian type telescope (28 cm in diameter) and a multichannel detector (Zieliński et al. 1994, 1997, Zieliński & Zieliński 1997). Each measuring session was preceded by a measurement of the initial power of the dye laser. Then, the wavelength of the laser operation was adjusted by changing the dye. The system is adapted for field work, and can be mounted on a car, a ship or an aircraft.

The aerosol concentration at an any altitude above sea level may be determined using the Potter procedure (1987) and the Mie algorithm, if a predetermined function is assumed. This procedure allows for the determination of extinction at an arbitrary point z_i located on the sounding path with lidar radiation of wavelengths λ_1 and λ_2 .

The Potter algorithm was used since it is the default in the FLS-12 lidar software. The optical depth within the distance range used in the research is so small that extinction could in fact be disregarded and multiplication by the square of the distance would be a sufficient algorithm. Therefore, deviations from the Potter algorithm do not significantly influence the results.

Non-linear minimization was used to determine the parameters describing the size distribution and the total aerosol concentration at particular altitudes h_i for particles in the radius range of $r \in [r_1; r_2]$. The values of radii r_1 and r_2 were derived theoretically using the Mie code and on the assumption that the aerosol ensemble consists of spherical particles with known optical properties (refraction index). A detailed description of the FLS-12 lidar and the measurement methodology can be found in Zieliński & Zieliński (2002).

The lidar-obtained aerosol concentrations were calibrated with those acquired from simultaneous measurements with a laser particle counter (CSASP-HV-100) (Zieliński 1998, Zieliński et al. 1998). The aerosol concentrations were calculated with a simple algorithm assuming a constant size distribution shape ($b = 2.0 \mu\text{m}^{-1}$, a typical value in the laser particle counter measurements). A detailed description of these calculations can be found in Piskozub et al. (1994).

3. Results

The experimental results obtained for the coastal zone in Athens are presented in Figs 3–8 in the form of plots illustrating the concentration of aerosol pollution as a function of altitude in different seasons of the year.

The results of a few thousand measurements have been analyzed, but only about a hundred representative ones have been chosen for further study. The measurements were typically performed in certain time ranges: between 10 and 12 a.m., between 10 a.m. and 2 p.m., and between 4 and 6 (sometimes 7) p.m. They were not made at night or at weekends, so it was not possible to determine the background level of pollution and the real increase in pollution during the day. Despite this, many interesting phenomena taking place in the troposphere were detected, thereby demonstrating its dynamism. The figures present the data for an altitude limited to 3000–4000 meters, because of the rapid decrease in the signal reaching the detector and an increase in detector noise for higher altitudes. The plots of the aerosol concentration versus altitude often reveal two maxima indicating the limits of the temperature inversion phenomenon. They also testify to the presence of a limiting layer of inversion, dependent on wind direction. The limit occurring below 2000 meters is indicative of the predominant effect of onshore winds, and the limit above 2000 meters – of the predominant effect of offshore winds. The direction of the wind also determines the type of aerosol in the troposphere. When the wind blows in from the sea (southerly, south-westerly direction) the aerosol is of the marine-urban type. In Athens the aerosol is not a purely marine type as the city is bordered on the south by the busy harbour of Piraeus and by densely urbanized areas, which supply enough pollution to change the composition of the aerosol recorded over the city. The winds blowing from the land carry a typical urban aerosol with small grains. The results obtained with the equipment of the Institute of Oceanology PAS in Sopot were not analyzed with the use of a general algorithm for calculating marine aerosols as the range of distances was small and did not exceed 200 meters. The restriction of this range was due to the limited visibility on the day of measurements; when the visibility was good, measurements were made up to altitudes of 500 meters. Iteration requires at least one thousand points, but since this could not be achieved even in very good weather, no iteration was performed. None the less, the data from Kołobrzeg are presented for the sake of comparison; in Athens it was impossible to measure aerosols of a purely marine type because of the character of the buildings and the city's location. Preliminary analysis of the results from Athens obtained on May 19, 2000 indicate a significant effect of the wind from the sea on the inversion layer, with the aerosol concentration reaching a maximum at an altitude of 465–510 meters (Fig. 3). The rate of ascent of the aerosol pollutants was low, about 1.5 meters per minute. The ascent was accompanied by an almost

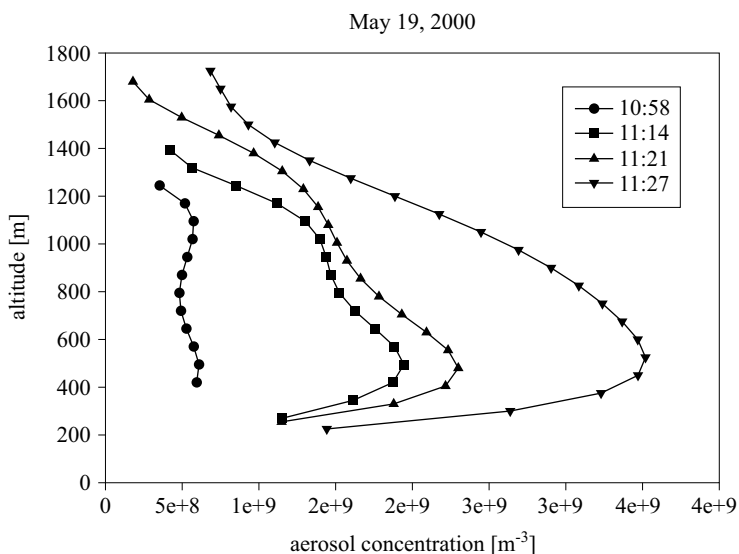


Fig. 3. The vertical dependence of aerosol concentration calculated in the morning of May 19, 2000, in Athens (concentration error – c. 10%)

8-fold increase in the concentration of pollutants. The size distribution of the aerosol grains also changed, and the sizes of the grains became smaller with time. At an altitude of about 1200 meters, the same influence of the wind from the land was observed. This land wind weakened with time and disappeared at about 11:30 a.m., whereas the wind from the sea strengthened and then dominated. The data from Athens of May 25, 2000, indicate a strong effect of the wind from the sea on the aerosol layer in the late afternoon. The inversion layer was at altitudes from 900 to 1000 meters and descended at a rate of 4 meters per minute. In this layer the concentration of pollutants increased by about a factor of two during the measuring session (Fig. 4). The data collected on August 25, 2000, indicate the effect of the wind from the land. There were two distinct inversion maxima, at altitudes of about 2000 and 4000 meters. The data shown in Fig. 5 provide evidence for a gradual increase in the concentration of pollutants (this increased two or three times), and the ascent of the two inversion maxima at a rate of about 2.5 meters per minute. The observations on September 10, 2000, indicate the occurrence of a maximum aerosol concentration at an altitude of about 1500 meters, at which the inversion layer occurs. The layer remained at the same level but the concentration of pollutants changed (Fig. 6). In the afternoon the concentration increased at 4.40–5.00 p.m., and then decreased again at 5.10–6.00 p.m. On November 3, 2000, the wind from the land

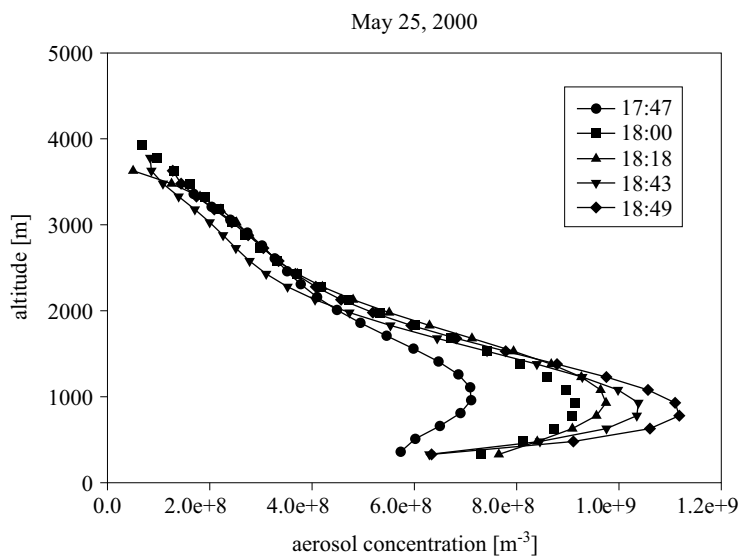


Fig. 4. The vertical dependence of aerosol concentration calculated in the afternoon of May 25, 2000, in Athens (concentration error – c. 10%)

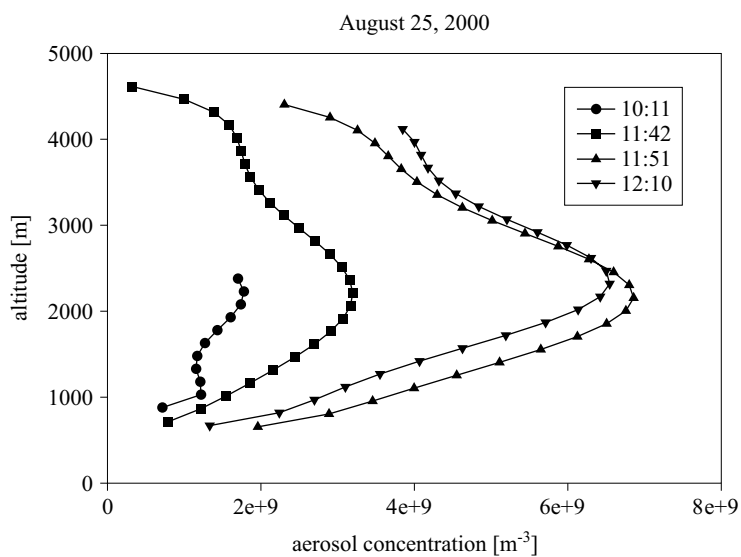


Fig. 5. The vertical dependence of aerosol concentration calculated in the late morning of August 25, 2000, in Athens (concentration error – c. 10%)

was dominant and caused a high rate of ascent of the inversion layer of 11 meters per minute. Simultaneously, the concentration of the aerosol pollutants increased by 2.5 times in the relatively short time of 40 minutes

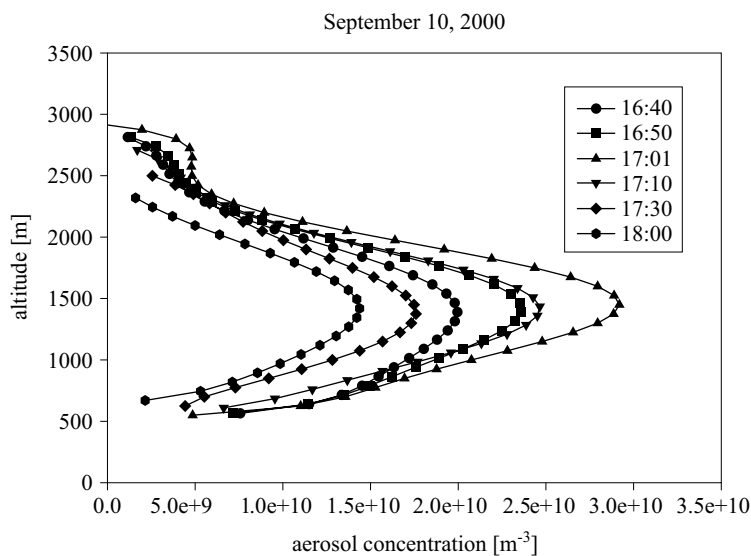


Fig. 6. The vertical dependence of aerosol concentration calculated in the late afternoon of September 10, 2000, in Athens (concentration error – c. 10%)

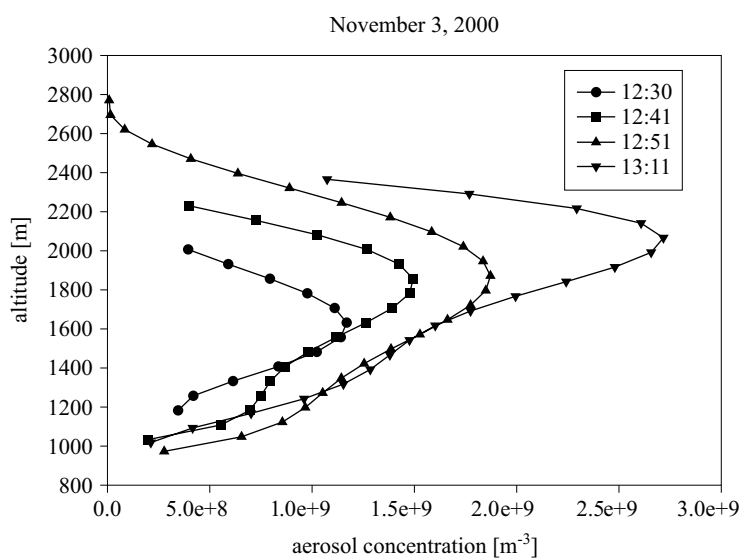


Fig. 7. The vertical dependence of aerosol concentration calculated in the afternoon of November 3, 2000, in Athens (concentration error – c. 10%)

(Fig. 7). The region where pollutants were present expanded from an altitude of ~ 1600 to ~ 2000 meters. On November 4, 2000, there was a strong wind from the sea and no wind from the land. The maximum of the inversion

layer (Fig. 8) ascended from 730 to 1100 meters at a rate of about three meters per minute.

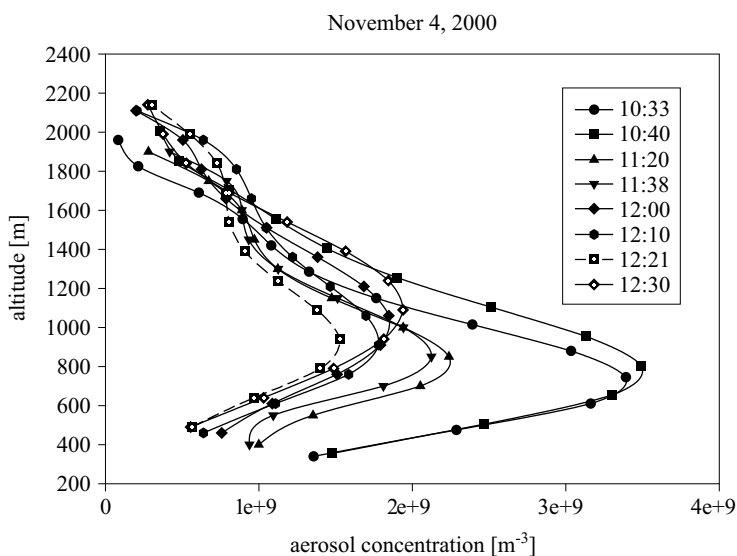


Fig. 8. The vertical dependence of aerosol concentration calculated at noon of November 4, 2000, in Athens (concentration error – c. 10%)

The plots in Figs 9 and 10 illustrate the concentration of the aerosol pollutants as a function of distance from the land measured in Kołobrzeg for offshore and onshore winds. The results suggest that the marine aerosols are characterized by a smaller extinction coefficient than those of urban origin. This is a consequence of the different refractive indices of the two types of particles. For pure marine aerosols, the maximum of the inversion layer occurs at about 60 meters just above the sea shore. However, little can be said about the aerosols occurring when the wind blows from the land, as there is then no distinct maximum of the inversion layer. The concentration of the purely marine aerosol was impossible to determine because the wind carried well mixed aerosol grains of high concentrations; however, it could be concluded that the aerosol concentration remained at the same level (Fig. 10) and was higher than when the wind was blowing in from the sea.

4. Discussion and conclusions

For winds blowing in from the sea in Kołobrzeg the inversion layer occurs at low altitudes from 40 to 60 meters (Fig. 9), in Athens at higher altitudes from 700 to 2000 meters (Figs 3–10). The inversion maxima are

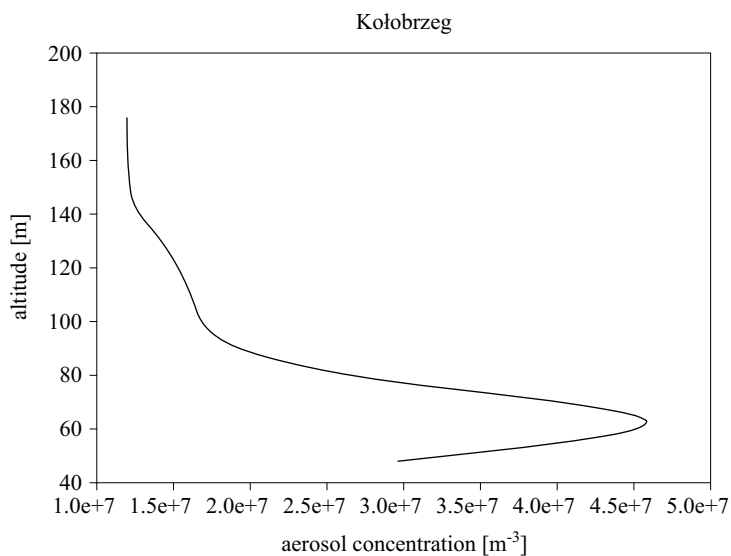


Fig. 9. The vertical dependence of aerosol concentration for onshore winds in the marine boundary layer of Kołobrzeg (concentration error – c. 10%)

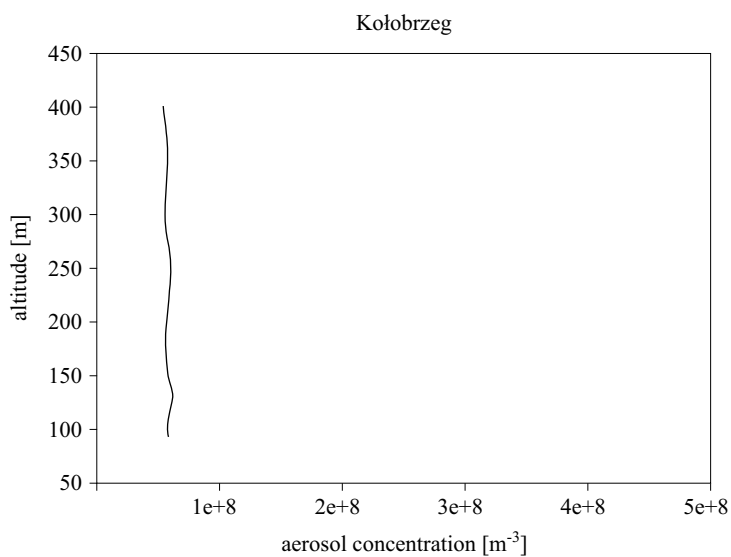


Fig. 10. The vertical dependence of aerosol concentration for offshore winds in the marine boundary layer of Kołobrzeg (concentration error – c. 10%)

narrow because the aerosol was chemically uniform, not a mixture containing pollutants from the land (Figs 4 and 9). For Athens the results indicated the presence of a second inversion maximum at altitudes above

2000 meters, testifying to the presence of terrigenous aerosols. The presence of such aerosols extends the lower inversion layer as a result of air currents and convection winds causing the interpenetration of terrigenous and marine aerosols. Owing to the long-lasting and intense mixing of these two types of aerosols, the inversion layer can be almost invisible, as seen in Fig. 10 (Kołobrzeg) (the effect of the land winds is noted). This phenomenon may be related to the morphology of the landscape, since Kołobrzeg, unlike Athens, is certainly not shielded from the land. Athens is surrounded by hills, which hinders the mixing of local marine aerosols with land aerosols; only in the late afternoon, when descending winds appear, are these two types of aerosols mixed. In Athens a mixture of the marine aerosol and the aerosol is formed as a result of solid fuel combustion; however, when onshore winds are strong the marine aerosols dominate. The data collected in Athens and presented in Figs 3–10 reflect the intense city traffic between 7 and 9 a.m. and between 4 and 6 p.m. The exhaust gases lead to the formation of an inversion layer at altitudes of 700–2000 meters (when the winds blow from the sea) and at altitudes above 2000 meters (when the winds blow from the land). The rate of ascent of the inversion layer depends on the intensity of sunlight, the strength of the wind and the structure of the landscape. The ascent is also influenced by the convection currents generated by thermal processes (an increase in solar energy reaching the land surface during the day). In the evening, the short-wavelength radiation from the sun ceases to reach the land, and the land cools by long-wave back-radiation from the earth, so that the inversion layer and the adjacent masses of air cool down. This causes the inversion layer to descend and the consequent increase in the concentration of pollutants in the near-ground layer, even though the intensity of traffic is now not so high.

Analysis of the aerosol concentrations versus altitude, in particular the altitude of the limiting layer, has shown that the altitude of the inversion layer of aerosols depends on the intensity of sunlight, and thus on the air temperature. This conclusion is illustrated in Fig. 11, which shows the data from Figs 3–10. The highest altitudes of the inversion maxima are observed in summer (July, August); they are lower in June and September and lowest in November. For aerosols carried by the winds from the land the maximum of the inversion layer was observed at 4000 m in summer and at 1500 m in autumn. For aerosols carried by the winds from the sea the maximum of the inversion layer occurred at 1500 m and 700 m in summer and autumn, respectively. The difference follows from the fact that the winds from the sea are usually cooler than those from the land. The difference in temperatures is also the reason why the altitudes of the inversion layer are lower in

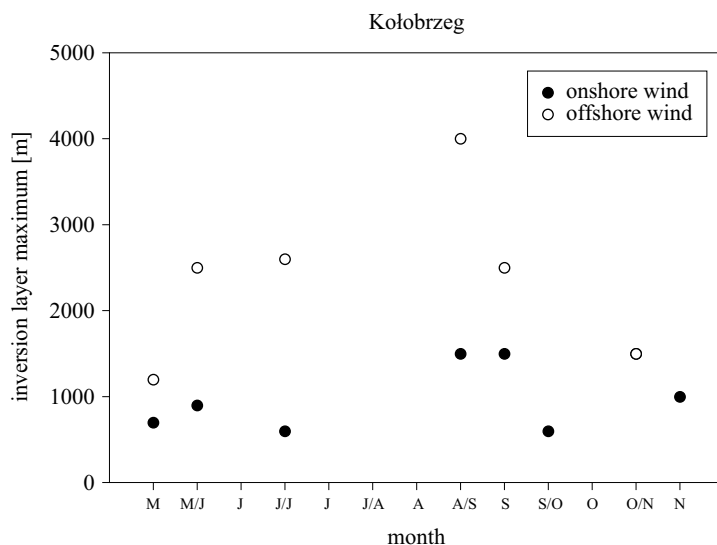


Fig. 11. The maximum inversion of the aerosol as a function of time for Athens in 2000

Kołobrzeg than in Athens; on the Baltic coast, temperatures are in general lower than in the Mediterranean. Atmospheric models need a reliable and easily obtainable indication of air mass characteristics for the determination of aerosol size distributions, concentrations and extinction in coastal areas, where a wide variety of rapidly changing atmospheric conditions have an impact on the aerosol ensemble. The results obtained using the lidar under similar meteorological conditions in various regions can be compared and used to determine the impact of regional and meteorological conditions on the concentration and shape of aerosol size distributions.

Acknowledgements

The NTUA lidar group was financed by the European Union (EAR-LINET Project).

References

- Ailisto H., Kostamovaara J., Lammasniemi J., Myllylä R., 1996, *Lidar measures up*, *Photon. Spectra*, 30 (3), 96–100.
- Błaszczak Z., Hałas M., Grabowski J., Papayannis A., 2003a, *Lidar study of the dynamics of aerosol type pollution in the lower troposphere over urban area*, *Proc. SPIE*, 5229, 51–53.

- Błaszczak Z., Hałas M., Grabowski J., Zieliński T., Papayannis A., 2003b, *A lidar study of aerosols in the lower troposphere over coastal regions in Poland and Greece*, Proc. SPIE, 5229, 54–57.
- Brinkmann U., 1999, *White-light pulsed lidar checks atmosphere*, Laser Focus World, 11, 36–38.
- Dixon G. J., 1998, *Laser radars produce three-dimensional pictures*, Laser Focus World, 34 (8), 129–136.
- Drollette D., 2000, *Ancient writings come to light*, Photon. Spectra, 4, 40 pp.
- Grabowski J., Papayannis A., 1999a, *Environmental sensing and applications*, Proc. SPIE, 3821, 12–18.
- Grabowski J., Papayannis A., 1999b, *Komunikaty VI Sympozjum Techniki Laserowej. Szczecin-Swinoujście 1999*, Wyd. Uczel. Politech. Szczec., Szczecin.
- Heintzenberg J., Tuch T., Wehner B., Wiedensohler A., Wex H., Ansmann A., Mattis I., Müller D., Wendisch M., Eckhardt S., Stohl A., 2003, *Arctic haze over Central Europe*, Tellus B, 55 (3), 796–807.
- Hong C. S., Lee K. H., Kim Y. J., Iwasaka Y., 2004, *LIDAR measurements of the vertical aerosol profile and optical depth during the ACE-Asia 2001 IOP, at Gosan, Jeju Island, Korea*, Environ. Monit. Asses., 92 (1)–(3), 43–57.
- Hoppel W. A., Fitzgerald J. W., Larson G. E., 1985, *Aerosol size distributions in air masses advecting off the East Coast of the United States*, J. Geophys. Res., 90, 2365–2379.
- Klett J., 1985, *Lidar inversion with variable backscatter/extinction ratios*, Appl. Optics, 24 (11), 1638–1643.
- Kovalev V. A., 1993, *Lidar measurements of the vertical aerosol extinction profiles with range-dependent backscatter to extinction ratios*, Appl. Optics, 32 (30), 6053–6065.
- Kunz G. J., de Leeuw G., Becker E., O'Dowd C. D., 2002, *Lidar observations of atmospheric boundary layer structure and sea spray aerosol plumes generation and transport at Mace Head, Ireland (PARFORCE experiment)*, J. Geophys. Res., 107 (D19), 8106, doi: 10.1029/2001JD001240.
- Labow G., Flynn L. F., Rawlins M. A., Beach R. A., Simmons C. A., Schubert C. A., 1996, *Estimation of ozone with total ozone portable spectroradiometer instruments. II Practical operation and comparisons*, Appl. Optics, 35 (30), 6084–6089.
- Marenco F., Santacesaria V., Bais A., Balis D., Di Sarra A., Papayannis A., Zerefos C., 1997, *Optical properties of tropospheric aerosols determined by lidar and spectrophotometric measurements (PAUR Campaign)*, Appl. Optics, 36 (27), 6875–6886.
- Measures R. M., 1984, *Laser remote sensing*, Wiley & Sons, New York, 217 pp.
- Mims F. M., 1992, *How to measure the ozone layer*, Sci. Probe 2, 4, 45–51.
- Mody S. E., 1999, *From earth to space, lasers take on pollution*, Photon. Spectra, 10, 96–103.

- Monahan E. C., Mac Niocaill G., 1986, *Oceanic whitecaps and their role in air-sea exchange processes*, D. Reidel, Dordrecht, 129 pp.
- Monahan E. C., Spiel D. E., Davidson K. L., 1983, *Model of marine aerosol generation via whitecaps and wave distribution*, Preprint vol., pp. 147–158, 9th Conf. 'Aerospace and Aeronautical Meteorology of the AMS', Omaha.
- Piskozub J., Petelski T., Król T., Marks R., Chomka M., Zieliński T., 1994, *A comparison of several measurement techniques used in BAEX'93 marine aerosol experiment*, Vol. I, pp. 36–43, Proc. 19th Conf. Baltic Oceanogr., Sopot.
- Resso M. J., Harris R. J., 1989, *A potpourri of infrared detector applications. Infrared detectors are routinely used in a host of applications*, Laser Optron., 1, 77–88.
- Robinson K., 2001, *Mobile Raman targets chemical spills*, Photon. Spectra, 2, 24 pp.
- Salemink H. W. M., Schotanus P., Bergwerff J. B., 1984, *Quantitative lidar at 532 nm for vertical extinction profiles and the effect of relative humidity*, Appl. Phys., 34, 187–189.
- Voss K. J., Welton E. J., Quinn P. K., Johnson J., Thompson A. M., Gordon H. R., 2001, *Lidar measurements during Aerosols 99*, J. Geophys. Res., 106 (D18), 20821–20831.
- Wilczak J. M., Gossard E. E., Neff W. D., Eberhard W. L., 1996, *Ground-based remote sensing of the atmospheric boundary layer: 25 years of progress*, Bound.-Lay. Meteorol., 78, 321–78, 349.
- Wu J., 1992, *Bubble flux and marine aerosol spectra under various wind velocities*, J. Geophys. Res., 97, 2327–2333.
- Zieliński T., 1998, *Changes in aerosol concentration with altitude in the marine boundary layer in coastal areas of the southern Baltic Sea*, Bull. PAS, Earth Sci., 46 (3)–(4), 133–139.
- Zieliński T., Chomka M., Piskozub J., Petelski T., 1998, *Verification of different techniques for the measurement of marine aerosols in coastal areas*, J. Aerosol Sci., 29 (Suppl. 1), 853–854.
- Zieliński A., Piskozub J., Zieliński T., 1994, *Lidar method in investigations of marine aerosols*, Bull. PAS, Earth Sci., 42 (1), 77–88.
- Zieliński T., Zieliński A., 1997, *Aerosol concentrations and their gradients near urban areas determined by means of the lidar method*, EurOpto Ser., Lidar Atmos. Monit., 3104, 242–247.
- Zieliński T., Zieliński A., 2002, *Aerosol extinction and optical thickness in the atmosphere over the Baltic Sea determined with lidar*, J. Aerosol Sci., 33 (6), 47–61.
- Zieliński A., Zieliński T., Piskozub J., 1997, *Aerosol size distribution function in the coastal area*, J. Aerosol Sci., 28 (Suppl. 1), 41–42.